Generation and classification of localized waves by Lorentz transformations in Fourier space

Peeter Saari and Kaido Reivelt
Institute of Physics, University of Tartu, Riia 142, 51014 Tartu, Estonia
(Received 15 August 2003; published 31 March 2004)

The Lorentz transformations of propagation-invariant localized waves (also known as nondispersive or nondiffracting or undistorted progressive waves) are studied in the frequency-momentum space. For supports of wave functions in this space rules of transformation are derived which allow one to group all localized waves into distinct classes: subluminal, luminal, and superluminal localized waves. It is shown that for each class there is an inertial frame in which any given localized wave takes a particularly simple form. In other words, any localized wave is nothing but a relativistically aberrated and Doppler shifted version of a simple ''seed'' wave. Also discussed are the relations of the physical (subluminal) Lorentz tranformation to other mathematical tranformations used in the literature on localized waves, as well as physical interpretation of the substantial changes that localized waves undergo if observed and generated in different inertial frames.

DOI: 10.1103/PhysRevE.69.036612 PACS number(s): 11.30.Cp, 42.25.Bs, 03.30.+p, 42.65.Re

I. INTRODUCTION

The exploration of ultrawideband subcycle or few-cycle pulsed fields has been expanding during the recent years hand in hand with advancements in the generation of ultrashort optical, terahertz, and ultrasonic pulses. The theoretical study of a specific subclass of such fields—beams of bulletlike wave packets called localized waves—was triggered by the discovery of several intriguing solutions to the linear source-free wave equation (see pioneering papers [1–11] and reviews [12–17]). The distinguishing feature of all types of the localized waves (LWs)-termed the Focus Wave Mode, *X* wave, Bessel-*X* and Bessel-Gauss pulses, etc.—is that their instantaneous intensity (or energy) distribution propagates without any spread or distortion in free space or linear media up to infinity in a theoretical limit. In reality, for finite-energy, i.e., finite-aperture waves, the depth of such an invariant propagation of the pulse—which, e.g., consists of an intense central peak with a diameter of the order of its mean wavelength on a sparse low-intensity background—is of course finite, yet it considerably exceeds the length of the waist of common focused wavefields. During the first 15 years of activity in theoretical research the ultrasonic *X* wave was the only LW whose feasibility had been verified [10]. Despite understandable obstacles encountered in the optical domain due to the large bandwidth and nonseparability inherent to LWs, to date optical *X*-type waves or Bessel-*X* pulses [18–22] and focus wave modes (FWMs) have been experimentally generated [23]. Very recently the formation of *X* waves in a nonlinear crystal was observed by an international research team [24]. A theory was developed for the propagation and diffraction of LWs in various optical elements and structures (see, e.g., Refs. [25,26] and references therein), in frequency doubling media [27], and optical parametric generators [28].

In a more general context LWs are related, on the one hand, to monochromatic (pseudo)nondiffracting beams, widely studied and applied since the intriguing paper on the zeroth-order optical Bessel beam [29]. In a sense an intermediate class is constituted by waveguide LWs composed of a discrete spectrum of harmonics of a waveguide mode [30]. On the other hand, continuous-spectrum superpositions of LWs [12,14] represent general finite-energy pulsed beams [31,32] that exactly obey the wave equation and consist of ultra-wide-band pulses converging to and expanding from the focus [33,34]. Finally, another generalization of the concept of propagation-invariant LWs leads to periodically self-reconstructing fields (see Refs. [15,35–37] and references therein).

Names of the LWs known so far—despite revealing some characteristics of a given LW—are of little help in systematizing the variety of them, all the more since the names are typically related to those LWs whose wave function has a particular closed-form mathematical expression, whereas the latter circumstance is rather occasional. A physical classification of LWs according to geometrical properties of the dependence between the frequency and longitudinal momentum of their monochromatic constituents was first introduced in Ref. [11]. This approach—actually based on considering the group velocity of the LW irrespective of its particular spectrum or wave function—has been developed further in our papers [38–42], where LWs are divided into classes depending on how the support of the spectrum looks in momentum space. Such a geometrical approach also reveals relationships between LWs hidden under different names. On the other hand, it turns out that the Lorentz transformation (LT) in coordinate-space relates the FWM to the well-known monochromatic Gaussian beam [6]. The coordinate-space LT has been used for developing the so-called boost representation of LWs [14], which not only relates some LWs to simpler waves considered in textbooks, but which also have helped to find new closed-form LWs.

In the present work we deal with Lorentz transformations in frequency-momentum space. The motivation is to develop a classification of LWs based on how the support of the spectrum behaves under the Lorentz transformation. Our aim is also to show how certain simple waves can be considered as parent or seed waves to families of LWs in the sense that any LW is nothing but an aberrated and Doppler shifted version of corresponding simple wave or, in other words, the latter observed in another inertial frame.

For introducing the main idea of the present study, let us

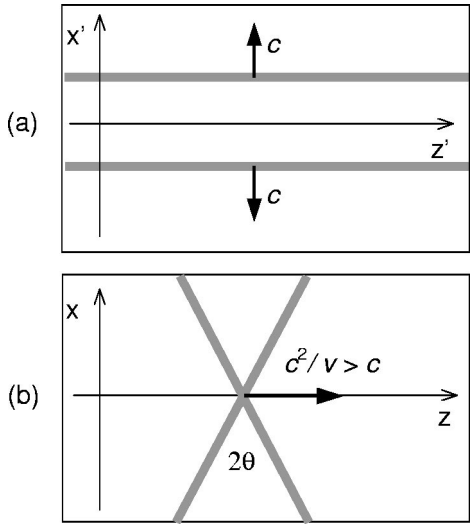

FIG. 1. Flight of two straights (depicted as thick grey lines) observed in different frames: (a) in the primed frame that moves to the right relative to the unprimed laboratory frame, and (b) in the unprimed frame that moves, conversely, to the left relative to the primed one.

consider a pair of straight lines which move—remaining parallel to the z' axis in an inertial reference frame K'—with a speed c in the (x',z') plane. The lines may represent, e.g., projections of phase or pulse fronts of plane waves that are perpendicular to the plane $(y'=0)$ [see Fig. 1(a)]. If at the moment $t'=0$ the lines coincide with the axis z', they are described by the equation $x'=\pm|ct'|$ while the coordinate z' is a freely running parameter for the lines. In a laboratory frame K, whose axes are parallel to those of K', and with respect to which K' is moving along the positive direction of the z axis with a subluminal speed v, the coordinates are given by the Lorentz transformations

$$x=x',$$

$$z=\gamma(z'+\beta ct'), \tag{1}$$

$$ct=\gamma(ct'+\beta z').$$

Here $\beta\equiv v/c<1$ is the speed of K' in units of c and $\gamma\equiv(1-\beta^2)^{-1/2}$. Through the use of Eq. (1) in the laboratory frame the equation of the moving lines turns out to be

$$x=\pm|\tilde{\gamma}(z-\beta^{-1}ct)|, \quad \tilde{\gamma}\equiv 1/\sqrt{\beta^{-2}-1}. \tag{2}$$

If one defines a superluminal speed $\tilde{v}\equiv\beta^{-1}c=c^2/v>c$, then $\tilde{\gamma}=(\tilde{v}^2/c^2-1)^{-1/2}$ turns out to be the superluminal counterpart of the relativistic factor γ. Equation (2) tells us that for a laboratory observer the lines behave in a completely different manner—instead of being parallel they are crossed under the angle $\theta=\operatorname{arccot}\tilde{\gamma}$ and the crossing point as well as the whole X-like figure moves along the z axis with the superluminal speed $\tilde{v}$, as shown in Fig. 1(b). (Parenthetically we remark that what one *observes* being in a reference frame is not what one *sees* or records by a camera, since the direct picture has been more or less distorted due to the finite time the scattered light needs to travel to the observer.) Hence, we have a hint that the X-type waves as well as other more complicated localized waves may be nothing but simple textbook-example-type waves observed from moving frames.

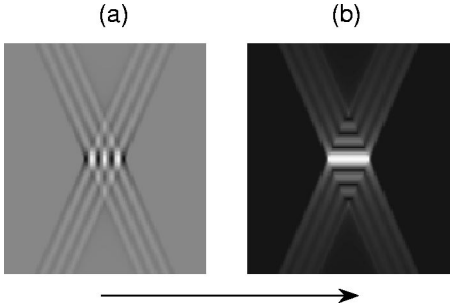

FIG. 2. Bessel-X wave field comprised of plane wave pulses containing about three cycles. As grey-scale plots in a plane of the propagation axis (the z axis) and at a fixed instant, shown are (a) the real part of the wave function and (b) its amplitude (modulus). The arrow indicates propagation direction of the wave.

To introduce the Fourier representation of LWs, let us consider a simple case of an axially symmetrical LW if not only its energy distribution (modulus squared of its wave function) but also the wave function itself is propagation invariant. In cylindrical coordinates and in the form of analytic signal it is given by a wideband superposition [$S(k)$ being the spectrum] of Bessel beams:

$$\Psi_X(\rho,z,t)=\int_0^\infty dk\, S(k)J_0(k_\rho\rho)\exp(ik_z z-i\omega t). \tag{3}$$

Here $k=\omega/c=2\pi/\lambda$ is the wave number, and ρ is the transversal distance from the propagation axis z. The zeroth-order Bessel function of the first kind $J_0(k_\rho\rho)$ can be viewed as a cylindrical counterpart of the lateral interference profile factor $\cos(k_\perp x)$ of the field of a pair of plane waves propagating with their $\mathbf{k}$ vectors in the (z,x) plane at angles $\pm\theta$ relative to the z axis. The component $k_\perp$ of the $\mathbf{k}$ vector is transverse to the z axis, $|k_\perp|\equiv k_\rho\equiv k\sin\theta$, and $k_z\equiv k\cos\theta$ is the wave number along the propagation axis. If such a LW does not contain low-frequency components down to the dc one, i.e., if $S(k\to 0)=0$, but the bandwidth Δk is still of the order of the mean wave number $\overline{k}$, the field shows both the Bessel-beam-type rings and the characteristic X-like shape in its spatial distribution (Fig. 2). Therefore such a LW has been called the Bessel-X wave [18]. Since $k_z z-\omega t=k_z(z-ct/\cos\theta)$, temporal dependence enters into Eq. (3) through the propagation variable $z_t=z-\tilde{v}t$ only, and therefore the whole pulse propagates rigidly along the z axis with superluminal speed $\tilde{v}\equiv c/\cos\theta$.

The paper has been organized as follows. In Sec. II we briefly introduce known general geometrical features of the Fourier representations of the localized waves, and derive some general rules that govern the impact of aberration and Doppler shift on the supports of the ultrawideband spectra of the LWs. In Sec. III we discuss superluminal generalizations

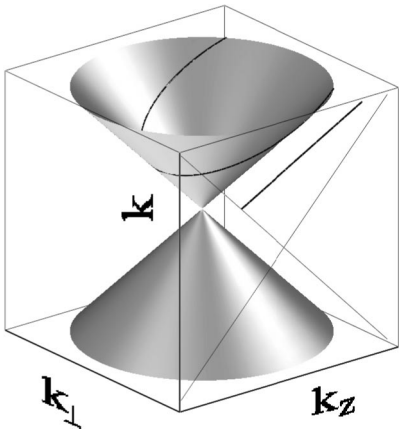

FIG. 3. The conical surface in the Fourier space, which the support of any wave has to lie on. The axis $k_\perp$ depicts one of the transverse components k_x, k_y or—for cylindrically symmetric waves—any transverse component of the wave vector **k**. Depicted on the surface is the support line of a localized wave, which has a subluminal velocity because—as seen in the figure—the projection of the line onto the (k_z,k) plane is a straight with a slope less than 1. Since for solutions to the wave equation as analytic signals the lower cone with negative frequencies is absent and for k_ρ representing the transverse components in the cylindrical system there are no negative values, henceforth we deal with the rear-left half of the upper cone only.

of the common Lorentz transformation and its modifications. Section IV contains our main results; there we systematize LWs into families according to geometrical and Lorentz-transformational properties of their supports in frequency-momentum space, and present an example for each family, showing how an elementary simple wave field with a particular spectrum gives birth—through a change of the speed of the reference frame—to a more complicated LW with a corresponding spectral profile. The last section contains comments and conclusions on the results obtained in Sec. IV.

II. LORENTZ TRANSFORMATIONS AND SPECTRAL SUPPORTS

A. Peculiarities of spectral supports of localized waves

Despite a general solution $\Psi(\mathbf{r},t)$ of the free-space scalar wave equation depends on four coordinates x, y, z, and ct, its transform domain (k-space or spectral) representation $\tilde{\Psi}(\mathbf{k},\omega/c)$ has only three independent arguments due to the dispersion-relation restriction $k_x^2+k_y^2+k_z^2-(\omega/c)^2=0$ imposed by the wave equation. In other words, the four-vector $(\mathbf{k},k\equiv\omega/c)$ of a light wave is always an isotropic one. Thus, the spectral function $\tilde{\Psi}(\mathbf{k},k)$ is not equal to zero only on the surface of a cone given by equation $k^2=k_x^2+k_y^2+k_z^2$ in the four-dimensional Fourier space. In other words, the support of the function $\tilde{\Psi}(\mathbf{k},k)$ has to lie on that conical surface. In the case of azimuthal symmetry one can introduce the cylindrical coordinates by replacing $k_x^2+k_y^2\rightarrow k_\rho^2$ thus reducing the dimensionality of the support to 2 and gaining a possibility to depict the support as a conical surface in Fourier space with three axes: k_z, k_ρ, k (or ω/c); see Fig. 3. The general axisymmetric field as an analytic signal is then expressible as an expansion over the zeroth-order Bessel beams propagating both forward and backward along the z axis:

$$\Psi(\rho,z,t)=\int_{-\infty}^{\infty}dk_z\int_{|k_z|}^{\infty}dk\,\tilde{\Psi}(k_z,k)J_0(\sqrt{k^2-k_z^2}\rho)\times\exp(ik_z z-ikct). \tag{4}$$

Here the two-dimensional integration covers the area of projection of the support on the cone onto the plane (k_z,k) in contrast to the one-dimensional integration in Eq. (3) above. For $|\Psi(\rho,z,t)|^2$ to be propagation invariant, i.e., to depend on z and t through the propagation variable $z-v_g ct$, where v_g is a constant group velocity along z axis in units of c, the variables k and k_z must be bound linearly [38–43],

$$k=v_g k_z+b, \tag{5}$$

where b is a constant. Hence, the spectrum has to be singular and may be factorized in the following form:

$$\tilde{\Psi}(k_z,k)=S(k)\,\delta(k-v_g k_z-b)\Theta(k^2-k_z^2), \tag{6}$$

where $S(k)$ is any complex-valued function of one real positive variable and the Heaviside unit step $\Theta(x)$ has been introduced as a factor in order to allow the k integration in Eq. (4) to start from $k=0$ instead of $k=|k_z|$. Thus, for an axisymmetric wave packet to be a propagation-invariant LW, its spectral support must be a line of intersection of the cone surface by a plane perpendicular to the plane (k_z,k); see Fig. 3. The projection of the line onto the plane (k_z,k) is a straight with the slope v_g (Fig. 3). Let us notice that, if $b=0$ and if the pulse is superluminal with $|v_g|>1$, the support may stretch up to the origin $k=k_z=k_\rho=0$ (since in this case $\Theta(k^2-k_z^2)=\Theta[k_z^2(v_g^2-1)]=1$) and the expression for the field reduces to Eq. (3).

B. Lorentz transformation of wave vector

In order to study how a (scalar) wave field given in one system of coordinates changes if observed from another inertial reference frame, one may employ the Lorentz transformation of the space and time variables of the wave function. This the approach the authors of Ref. [14] is applied to derive various localized wave solutions to the wave equation. Alternatively, one may Lorentz transform the wave vectors of the single-frequency constituents of the field instead, and leave the coordinates alone as free variables. In this case the transformation of the field, including the change of its spatiotemporal shape, is considered as a manifestation of the distinct physical effects—the Doppler shift and the aberration. This is the approach we employ throughout the present study. The Lorentz transformations of the components of the wave vector read

$$\begin{aligned} k_\rho &\Rightarrow k_\rho,\\ k_z &\Rightarrow \gamma(k_z+\beta k),\\ k &\Rightarrow \gamma(k+\beta k_z). \end{aligned} \tag{7}$$

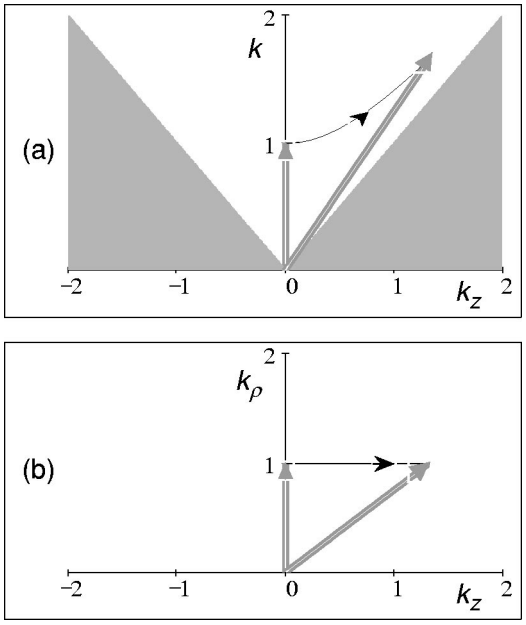

FIG. 4. Geometrical representation of the Doppler shift and aberration of a monochromatic plane wave as the Lorentz transformation of its wave vector. Depicted are the wave vector projections (grey double-line arrows) (a) onto the (k_z,k) plane and (b) onto the (k_z,k_ρ) plane. The unit of the scales is conventional but if it is taken to be 10^7 rad/m$=10$ rad/μm, values of k from 1 to 2 units fall into optical domain from red to near ultraviolet. The forbidden region outside the conical surface (cf. Fig. 3) is depicted by gray shading. Thin black lines with arrows indicate projections of the trajectory of the tip of the wave vector as the relative speed β between the reference frames increases from the initial value $\beta=0$ up to $\beta=0.8$. The initial vector, i.e., the vector in the frame K' (coinciding with the unprimed laboratory frame if $\beta=0$) has been taken—as an example—transverse to the z axis. The Doppler shift to the blue as observed in the laboratory frame is manifested (a) by growth of the vertical component of the vector in the (k_z,k) plane or, equivalently, (b) by increase of the length of the vector in the (k_z,k_ρ) plane.

Unlike Eq. (1) the primes have been omitted here and expression (7) is interpreted as follows: given a wave field in the moving frame K', we replace the wave vectors of its cylindrical-wave constituents in order to get the wave function describing the field, as observable in the laboratory frame. The transformation is geometrically depicted in Fig. 4. We see that as the relative speed between the frames changes, the end point of the wave vector projection draws a hyperbola in the (k_z,k) plane, while the change of the ordinate k of the point displays a Doppler shift and a change of the abscissa k_z (the aberration). Let us note parenthetically that the vanishing derivative of the curve near the vertical axis depicts the well-known quadratic smallness ($\sim\beta^2/2$) of the transverse Doppler effect.

Equation (7) and Fig. 4 also indicate how the k-domain support of a general axisymmetric field—see Eq. (4)—is transformed if the field is observed in another reference frame: every point of the support has to move along surface of the cone (Fig. 3) to a new location in accordance with Eq. (7). The most singular support is a single point—the tip of the wave vector—with fixed triplet of values of $k_z,k,k_\rho=\sqrt{k^2-k_z^2}$. Such a support corresponds to a monochromatic Bessel beam. So, Fig. 4 shows the transformation of a single-point support as well. It follows from Fig. 4 particularly that, for any monochromatic Bessel beam, there is an inertial frame where the longitudinal component k_z vanishes; consequently, in such a ''rest'' frame the beam becomes a z-independent cylindrical monochromatic standing wave with the wave function $J_0(\rho k)\exp(ikct)$.

C. Lorentz transformation of support lines

As indicated above, for a wave packet to be propagation invariant its support in the k space has to be degenerated into a line, the projection of which onto the (k_z,k) plane has to lie on a straightline. Henceforth, for brevity we shall use term ''support lines'' for such one-dimensional supports and their projections. In this subsection we consider some general rules that govern the transformation of the support lines of the localized waves, which will be useful for a classification of the waves in Sec. III. The lines as conical-section-type curves change their parameters but retain the type of the (generally curved) line, as will be deduced below from Eq. (7). We shall consider both projections of the support, onto the plane (k_z,k) and plane (k_z,k_ρ); see Fig. 3. The support line in the latter plane reveals well the composition of a given LW from plane wave constituents, e.g., a straightline in the plane (k_z,k_ρ) says that the LW consists of common plane wave pulses, whereas a curved line means that the constituents are tilted pulses [37].

In the plane (k_z,k) the line is straight given by Eq. (5) and, as the transformations [Eqs. (7)] are linear, the line remains straight, but its parameters are changed according to the following relations

$$v_g \Rightarrow \frac{(v_g+\beta)}{(1+v_g\beta)}, \qquad b \Rightarrow \frac{b}{\gamma(1+v_g\beta)}. \tag{8}$$

By taking appropriate limits in the right-hand side of expression (8)—the first row of which is nothing but the relativistic law for addition of velocities—we get the following rules.

(1) $v_g \Rightarrow \mathrm{sgn}(\beta)$ if $|\beta|\approx 1$, i.e., no matter what the group velocity along the pulse's propagation axis is in a given frame—equal to c (luminal) or sub- or superluminal, the localized wave turns out to be luminal if observed in another reference frame that moves extremely relativistically with respect to the first one.

(2) $v_g \Rightarrow \mathrm{sgn}(v_g)$ if $|v_g|\approx 1$, i.e., no matter what the speed of another reference frame is, a luminal localized wave is also luminal in it.

(3) A subluminal (superluminal) localized wave remains subluminal (superluminal) in any possible frame, except the first case is an extreme one.

(4) Also invariant is the condition $b=0$, which is possible only for superluminal localized waves—of course, if we do

not consider common luminal plane waves—and results in an equality of the phase and group velocities of the wave, as seen from Eq. (4).

To summarize, belonging to one of the distinct classes or ''families'' of localized waves—subluminal, luminal, generic superluminal or superluminal with a propagation-invariant wave function—is an invariant attribute of a localized wave. This invariance will be made use of in Sec. III for classification of the waves.

Considering projections of the support onto the plane (k_z,k_ρ), from Eq. (7) we notice first that in this plane in the course of the Lorentz transformation every point of the support moves along a straight parallel to the k_z axis. However, due to the nonlinear relation $k^2=k_\rho^2+k_z^2$ a support line given by Eqs. (5) and (6) is generally not straight in the (k_z,k_ρ) plane or does not remain such under the Lorentz transformation. The support line in this plane is generally a cone section instead, as is also obvious from Fig. 3. Only in a particular case, when $b=0$ in Eqs. (5) and (6), is the support a straight-line in both planes (k_z,k) and (k_z,k_ρ) simultaneously, and remains straight under the Lorentz transformation in which the slope $\alpha\equiv\tan\theta$ in the equation of the support line $k_\rho=\alpha k_z$ transforms in the following manner:

$$\tan\theta\Rightarrow\tan\theta\frac{\sqrt{1-\beta^2}}{1+\beta/\cos\theta} \tag{9}$$

if we use the Axicon angle θ under which all the plane wave constituents propagate in the given case; see Eq. (3). The shape of the support in the (k_z,k_ρ) plane gives an idea about the physical angular spectrum of the wave and possibilities to generate it.

III. RELATION TO OTHER TRANSFORMATIONS

A. Superluminal Lorentz transformations

In Ref. [14] the Lorentz transformation (LT) has been generalized by introducing a superluminal LT for the case of a superluminal speed $\tilde{v}$ of the frame, which in our designations reads

$$x=x',$$

$$z=\tilde{\gamma}(\tilde{\beta}z'+ct'), \tag{10}$$

$$ct=\tilde{\gamma}(\tilde{\beta}ct'+z'),$$

where $\tilde{\beta}\equiv\tilde{v}/c$ and $\tilde{\gamma}\equiv(\tilde{\beta}^2-1)^{-1/2}$; see Sec. I. The authors of Ref. [14] use this superluminal LT as if it generates new solutions to the scalar wave equation that are distinct from those they obtain by using the common subluminal LT. However, as one can make sure by setting $\tilde{\beta}=\beta^{-1}$, all the right-hand sides of Eq. (10) turn out to be equal to that of Eq. (1). So, the superluminal LT defined by Eq. (10) cannot give anything different, and we prefer to work solely by the common subluminal LT of 4 vectors, all the more since the coordinates in Eq. (10) remain unchanged weirdly only in an extremely superluminal case, i.e., if $\tilde{\beta}\to\infty$. Of course, if one applies the subluminal LT to a wave, it is not inconceivable that a superluminal velocity $\tilde{v}=c^2/v$ may appear in the expression of the transformed wave, as mentioned already in Sec. 3.2 of Ref. [14].

There is another superluminal version of the LT known mainly in tachyon research, which is defined like the common LT via Eq. (1), except that the quantities γ and β are replaced with their superluminal counterparts $\tilde{\gamma}$ and $\tilde{\beta}$. Let us note parenthetically that this replacement will *not* result in Eq. (10). However, the physical meaning of this transformation into ''tachyon world'' remains controversial, since it inverts the sign of the interval, i.e., changes timelike quantities into spacelike ones and vice versa; moreover, it loses a point-to-point correspondence between objects as observed in the moving and laboratory reference frames. It is interesting to note that thanks to the latter peculiarity the authors of Ref. [44] found that a tachyon should have a characteristic shape—essentially the same one we know now an *X*-type localized wave has; also see Refs. [17,45].

B. Lu-Zou-Greenleaf transformation

Lu, Zou, and Greenleaf [46] proved a theorem indicating how to get from a two-dimensional wave solution valid in the (x,y) plane to a three-dimensional solution rigidly moving along the z axis with superluminal speed. For that purpose one needs simply to replace the arguments $(x',y')\equiv\vec{\rho}'$ and t' of the two-dimensional wave function according to the following rules:

$$\vec{\rho}'=\vec{\rho}\sin\theta,$$

$$ct'=ct-z\cos\theta,$$

where $0<\theta<\pi/2$ is the angle introduced above as a characteristic of the shape and a measure of superluminality of an *X*-type wave. As scaling of all arguments by a constant—in particular, division by $\sin\theta$—does not change the source-free wave equation, the following transformation must do the same job as the Lu's does:

$$\vec{\rho}'=\vec{\rho},$$

$$ct'=\cot\theta\left(\frac{c}{\cos\theta}t-z\right)=\tilde{\gamma}(\tilde{\beta}ct-z).$$

However, the latter is an equivalent of Eq. (10), which in turn was nothing but the common subluminal Lorentz transformation. Hence, as already noted in Ref. [14], the Lu transformation is a particular case of the Lorentz transformation and this is the reason why the theorem works. The Lu transformation has been successfully exploited by various authors for different purposes, e.g., for deriving *X*-shaped beams propagating in cylindrical waveguides from known planar wave solutions [30].

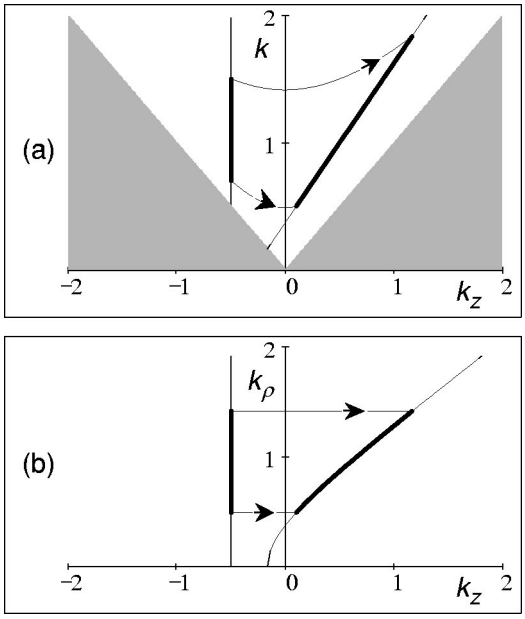

FIG. 5. The supports of superluminal localized waves and the relationship between them through the Lorentz transformation. The support lines are depicted as projections (a) onto the (k_z,k) plane and (b) onto the (k_z,k_ρ) plane. The support corresponding to infinite-group-velocity LWs, all plane-wave constituents of which have the same value $k_{z0}=-0.5$ of the longitudinal component of their wave vector, have been chosen as the initial support observed in the frame K' (or also in the laboratory frame K if $\beta=0$). The final shape of the support (in the laboratory frame) has been depicted for $\beta=0.8$. The thick black line depicts the support of a band-limited LW, while the thin line beneath it depicts the supports of all possible LWs with given group velocity. Concerning the units and other explanations, see the previous figure caption.

IV. GENEALOGY OF LOCALIZED WAVES

All localized waves belong to one of the three families—superluminal, subluminal, and luminal—according to the slope of the straight representing the support in the plane (k_z,k). Inside each family the LWs differ—besides values of the support parameters v_g and b; see Eq. (6)—by their particular one-dimensional spectrum $S(k)$ along the support line: it may be more or less wide band, may or may not result in a closed-form expression for $\Psi(\rho,z,t)$ according to Eq. (4), etc. However, all waves with similar shapes (scaling may differ) of the spectrum can be considered as one and the same, no matter what the particular value of the subluminal or superluminal velocity is, since all these waves are related through the LT. In other words, all these waves are one and the same, but observed in different reference frames. If this is the case, a reference frame should exist where the wave has the simplest form. Such a wave can be considered as a ''seed'' for corresponding localized waves. In this main section of the paper we show that the ''seed'' waves have infinitely large or vanishing values of the group velocity.

A. Generic superluminal family

The tranformation of the support lines, as analyzed in Sec. II C, is illustrated graphically in Fig. 5. We see that the straight lines, whose slope in the (k_z,k) plane exceeds a value 1 by its absolute value, are LT replicas of each other, while the projection of the same superluminal support line onto the (k_z,k_ρ) plane is generally a hyperbola. Of particular interest is the support line with a fixed value of k_z, in which case the group velocity is infinitely large. We have chosen this to be the case in the moving frame K'. Hence, according to Fig. 5(a) the larger the speed of the frame the smaller the group velocity of the wave in the laboratory frame. However, the velocity retains its superluminality. Only if the speed of the frames relative to each other attains its limiting value c ($|\beta|\to 1$); the group velocity decreases to c or $|v_g|=1$.

Let us consider a particular spectrum—an ultrawideband one with exponential decay toward higher frequencies, i.e., let Eq. (6) take the form

$$\tilde{\Psi}(k_z,k)=e^{-k\Delta}\delta(k_z-k_{z0})\Theta(k^2-k_z^2) \tag{11}$$

in the frame K', where Δ is a positive constant characterizing the length of the wave pulse ($\Delta\to 0$ for a white spectrum), k_{z0} is the fixed value of k_z and the primes referring to variables in K' have been omitted for brevity. Inserting Eq. (11) into Eq. (4) and integrating over k_z contained in the δ function, one obtains

$$\Psi(\rho,z,t)=\exp(ik_{z0}z)\int_{|k_{z0}|}^{\infty} dk\, J_0(\sqrt{k^2-k_{z0}^2}\rho) \times\exp[-k(\Delta+ict)]. \tag{12}$$

The integral can be taken with the help of any Laplace transform table [e.g., Eq. 4.15(9) in Ref. [47]] and the wave obtains a simple form

$$\Psi(\rho,z,t)=\frac{\exp(-|k_{z0}|\sqrt{\rho^2+(\Delta+ict)^2})}{\sqrt{\rho^2+(\Delta+ict)^2}}\exp(ik_{z0}z), \tag{13}$$

i.e., it turns out to be a simple cylindrical pulse modulated harmonically in the axial direction and radially converging to the axis and thereafter expanding from it, the intensity distribution resembling an infinitely long tube coaxial with the z axis and with time-dependent diameter; see Fig. 6. To our best knowledge, this wave was first considered as a localized wave of infinite group velocity in Refs. [38,42]. This cylindrical wave is a ''seed'' one for all superluminal localized waves possessing the exponential spectrum, as we will see by redoing the derivation for the laboratory frame variables. Inserting Eq. (11) into Eq. (4) for the laboratory frame, we bear in mind that under the integral Lorentz invariants are $k_z z-kct$, $k^2-k_z^2$, and $dk_z dk$, while, according to Eq. (7),

$$e^{-k\Delta}\delta(k_z-k_{z0})\Rightarrow\exp[-\gamma(k-\beta k_z)\Delta] \times\gamma^{-1}\delta(k_z-\beta k-k_{z0}/\gamma). \tag{14}$$

The new argument of the δ function obeys the relations considered in Sec. II C. Performing the integration over k_z now complicates the arguments of the Bessel and Heaviside functions:

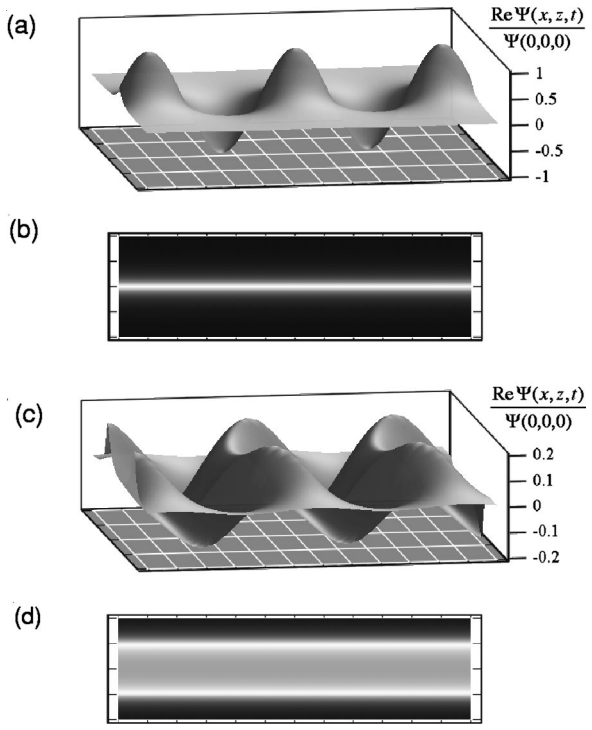

FIG. 6. The cylindrically converging-expanding wave given by Eq. (13). Shown are the dependences [(a) and (c)] of the real part and [(b) and (d)] of the modulus of the wave function on the coordinate z (increasing from the left to the right) and on a transverse coordinate $x=\pm\rho$ at two time instants: [(a) and (b)] $ct=0$ and [(c) and (d)] $ct=1/10$ μm. The distance between the grid lines on the basal plane (x,z) is 1/10 μm. The chosen values of the parameters are $\Delta=1/80$ μm and $k_{z0}=-2\pi/\lambda$ with $\lambda=1/2$ μm (the plots remain the same with any other unit length instead of 1 μm). The grey-scale plots of $|\Psi(x,z,t)|$ are normalized to "white" at the plot maximum, so that the "white" level in the plot (d) is actually five times weaker than in plot (b). The grey shading in plots (a) and (c) is a result of "lighting" used for better revealing the relief of the surface.

$$k^2-k_z^2 \Rightarrow k^2-(\beta k+k_{z0}/\gamma)^2;$$

however, the resulting integral over k can be given the same familiar form [Eq. 4.15(9) in Ref. [47]] by change of the variable $k\Rightarrow\gamma(k+\beta k_{z0})$ and we finally obtain

$$\Psi(\rho,z,t)=\frac{\exp(-|k_{z0}|\sqrt{\rho^2+[\Delta-i\gamma(\beta z-ct)]^2})}{\sqrt{\rho^2+[\Delta-i\gamma(\beta z-ct)]^2}} \times\exp[i\gamma k_{z0}(z-\beta ct)]. \quad (15)$$

This wave differs from that given by Eq. (13) qualitatively in the same manner as Fig. 1(b) from Fig. 1(a) in Sec. I; see Fig. 7. Of course, Eq. (15) can be derived from Eq. (13) by the LT of the coordinates given by Eq. (1) as well. Earlier this type of localized wave was derived and studied theoretically in Ref. [14] from what the authors term "superluminal boost representation" and in Ref. [48] by another general approach based on complex space-time ray theory. The authors of Ref. [14] called it a "focused X wave" (FXW), since

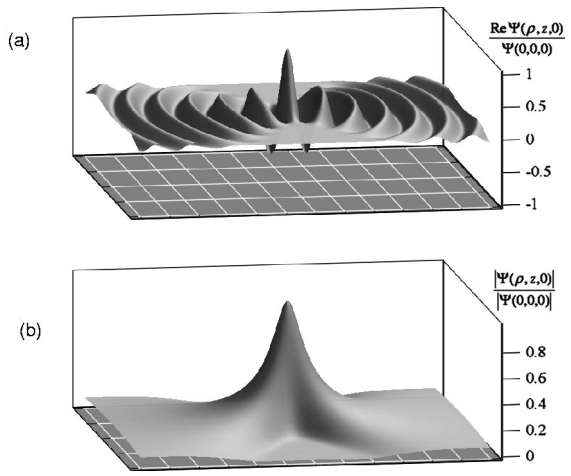

FIG. 7. The superluminal FXW given by Eq. (15) or (16). Shown are the dependences (a) of the real part and (b) of the modulus of the wave function on the longitudinal and transverse coordinates. The distance between the grid lines on the basal plane (x,z) is 1/10 μm. Chosen values of the parameters are $\Delta=1/15$ μm and $k_{z0}=-2\pi/\lambda$ with $\lambda=1/30$ μm and $\beta=0.8$ or $\tilde{v}=1.25c$. Also see the previous figure caption.

the wave resembles to a certain extent both the FWM and the X-type waves. For a better comparison with the X wave expression in Sec. IV B and with Eq. (4.4) of Ref. [14] we rewrite Eq. (15) using the superluminal quantities $\tilde{v}$ and $\tilde{\gamma}$ [see Eqs. (2) and (10) and the text after them]:

$$\Psi(\rho,z,t)=\frac{\exp(-|k_{z0}|\sqrt{\rho^2+[\Delta-i\tilde{\gamma}(z-\tilde{v}t)]^2})}{\sqrt{\rho^2+[\Delta-i\tilde{\gamma}(z-\tilde{v}t)]^2}} \times\exp\left[i\tilde{\gamma}k_{z0}\left(\frac{\tilde{v}}{c}z-ct\right)\right]. \quad (16)$$

The FXW has a tight (exponential) transversal localization but is yet an infinite-energy wave. Its intensity distribution (modulus squared) propagates invariantly with velocity $\tilde{v}>c$; however, the wave function itself has a fine modulational structure (see Fig. 7), copropagating or counterpropagating with luminal velocity depending on the sign of k_{z0}. Of course, the FXW represents only one possible superluminal localized wave, cylindrical waves with spectra which differ from that given by Eq. (13) give birth through LT to other superluminal waves that need not have closed-form mathematical expressions but all share the same general properties, in particular, the hyperbolic support of the angular spectrum in the (k_x,k_y,k_z)-space.

B. Subfamily of superluminal pulses with a propagation-invariant wave function

In case $k_{z0}=0$ the support line in both planes (k,k_z) and (k_ρ,k_z) lies on a straight which goes through the origin (Fig. 8), i.e., the hyperbolic support degenerates into a straightline. Hence, in the momentum space of the laboratory frame all wave vectors lie on the surface of a cone, or, in other words,

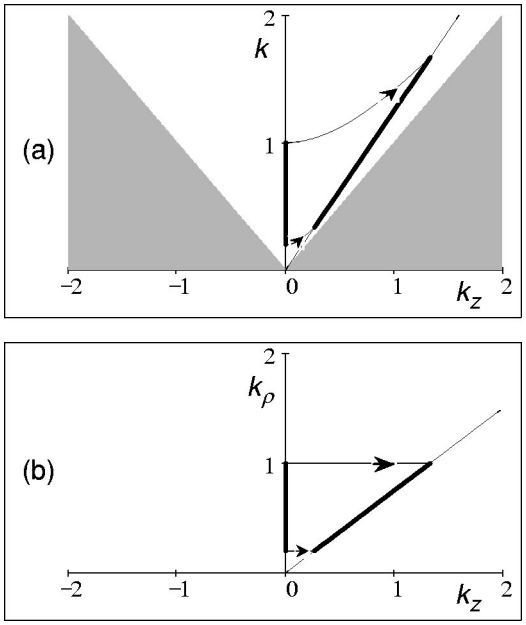

FIG. 8. The supports of superluminal localized waves with a propagation-invariant wave function, and the relationship between them through the Lorentz transformation. The shape of the support in the laboratory frame has been depicted for $\beta=0.8$ (see Fig. 5).

all plane-wave constituents of the LW propagate under the same fixed angle θ relative to the z axis and we recognize the superluminal X wave considered in Sec. I. The moving frame expression [Eq. (13)] reduces for $k_{z0}=0$ to

$$\Psi(\rho,z,t)=\frac{1}{\sqrt{\rho^2+(\Delta+ict)^2}}, \tag{17}$$

which represents a simple two-dimensional pulsed wave cylindrically converging to and expanding from the z axis like the modulus of the wave of the preceding subsection. In the laboratory frame, instead of Eqs. (15) and (16) we now obtain

$$\Psi(\rho,z,t)=\frac{1}{\sqrt{\rho^2+[\Delta-i\gamma(\beta z-ct)]^2}}$$

$$=\frac{1}{\sqrt{\rho^2+[\Delta-i\tilde{\gamma}(z-\tilde{v}t)]^2}}, \tag{18}$$

which are nothing but the fundamental X wave solutions known since pioneering papers [10] and [12]. Despite various plots depicting the X wave can be found in numerous papers, just for convenience and comparison we present one in Fig. 9. Had we taken another spectrum, e.g., $\tilde{\Psi}(k_z,k)=k^m e^{-k\Delta}\delta(k_z)\Theta(k)$ in Eq. (11), we would have obtained higher-order X waves [15] corresponding to mth-order derivatives with respect to time in Eq. (18). In any case, all X-type waves share the following main features: invariantly and superluminally propagating wave function, support lines

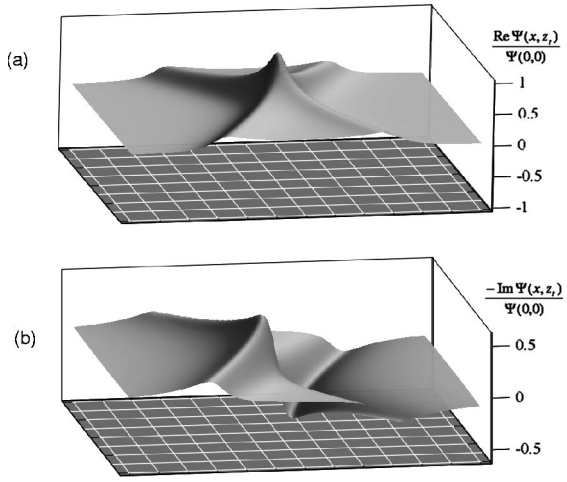

FIG. 9. The superluminal X wave given by Eq. (18). Shown are the dependences of the real (a) and imaginary (b) parts of the wave function on the propagation variable $z_t=z-\tilde{v}t$ and the transverse coordinate. The distance between the white grid lines on the basal plane is the same as in Fig. 7, but in the transverse direction the length scale has been compressed by factor of 2. Chosen values of the parameters are $\Delta=1/15$ μm and $\beta=0.8$ or $\tilde{v}=1.25c$.

are straights in both planes (k_z,k) and (k_z,k_ρ) and their prolongations cross the origin.

C. Subluminal family

As seen in Figs. 10 and 3, the support line of a subluminal LW—i.e., if the slope in the (k_z,k) plane is less than 1 by its absolute value—cannot cross the origin. Hence, for subluminal LWs, i.e., if $v_g<1$ the parameter b cannot vanish in Eqs. (5) and (6), and Eq. (8). We also see that the projection of any subluminal-type support line onto the (k_z,k_ρ) plane is generally an ellipse. Of particular interest is the support line with a fixed value of $k=b$, in which case $v_g=0$. Physically this is understandable as the spatial distribution of energy remains still for a strictly monochromatic field. Let such a rest frame be K'. According to Fig. 10(a) the larger the speed of the frame K', the larger the group velocity and the bandwidth of the wave in the laboratory frame. However, the wave retains its subluminality only if the speed of the frames relative to each other attains its limiting value c; the group velocity increases also to c.

In much the same way as in Sec. IV A, let us present an example showing how a "seed" wave possessing a simple form in its rest frame transforms into corresponding subluminal LW in the laboratory frame. We consider a particularly simple "seed" wave, a monochromatic spherical standing wave

$$\Psi(\rho,z,t)=\frac{\sin(br)}{br}\exp(-i\omega t), \quad r\equiv\sqrt{\rho^2+z^2}, \tag{19}$$

where the temporal frequency $\omega=cb$ corresponds to a monochromatic fixed value of $k=b$. Equation (19) has been normalized to a unit peak at the origin and the expression can

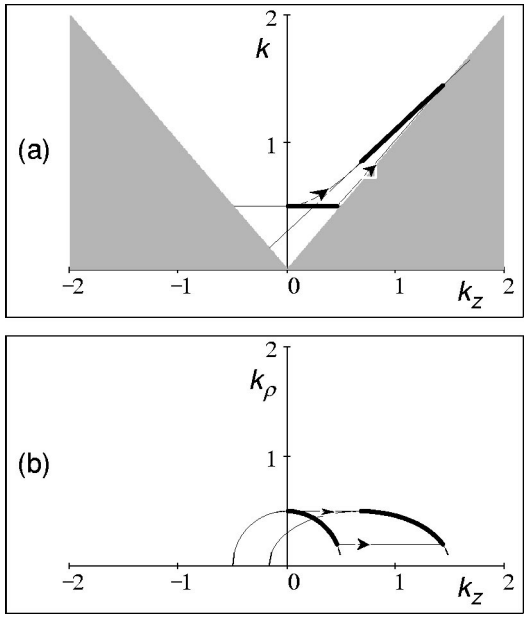

FIG. 10. The supports of subluminal localized waves and relationship between them through the Lorentz transformation. The support lines are depicted as projections (a) onto the (k_z,k) plane and (b) onto the (k_z,k_ρ) plane. The support corresponding to a monochromatic beam, all plane-wave constituents of which have the same frequency $\omega/c=b=-0.5$ and propagate in the positive direction of the z axis, have been chosen as initial support observed in the frame K'. This support and its Lorentz-tranformed equivalent in the laboratory frame with $\beta=0.8$ are depicted by the thick black line. The thin line beneath it depicts the supports of fields, plane-wave constituents of which propagate in both directions of the z axis, i.e., in all possible directions as it is in the particular case of fields given by Eqs. (19)–(22) (see Figs. 5 and 8).

be obtained as an isotropic superposition of plane waves propagating in all possible directions. For this wave Eq. (6) takes the form

$$\tilde{\Psi}(k_z,k)=\frac{2}{b}\delta(k-b)\Theta(k^2-k_z^2), \tag{20}$$

since inserting Eq. (20) into Eq. (4), and integrating with the help of a table of the Fourier transforms of the Bessel functions, returns the right-hand side of Eq. (19).

If we perform the same procedure for the laboratory frame, the support line has to be Lorentz-transformed (Fig. 10), i.e.,

$$\delta(k-b)\Rightarrow\delta(k-\beta k_z-b/\gamma)\gamma^{-1}. \tag{21}$$

Everything else under the sign of integration remains invariant; however, carrying out the integration over k now complicates the arguments of the Bessel and Heaviside functions:

$$k^2-k_z^2\Rightarrow(\beta k_z+b/\gamma)^2-k_z^2.$$

Again, the remaining integral over k_z can be given the same familiar form of the Fourier integral of $J_0(\sqrt{b^2-k_z^2}\rho)$ by change of the variable $k_z\Rightarrow\gamma(k_z+\beta b)$, and we finally obtain

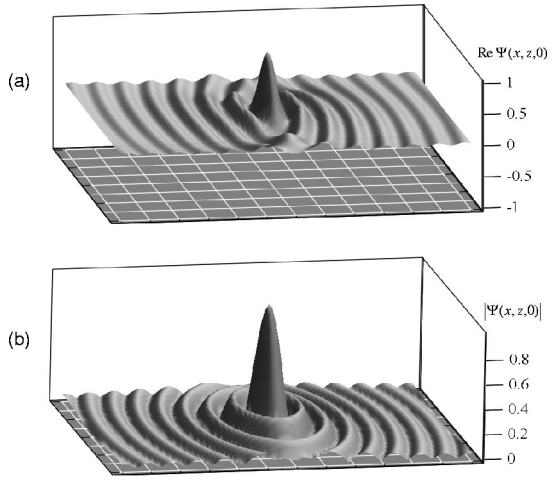

FIG. 11. The subluminal Mackinnon's pulse given by Eq. (22). Shown are the dependences (a) of the real part and (b) of the modulus of the wave function on the longitudinal and transverse coordinates. The distance between the white grid lines on the basal plane is the same as in Fig. 7, but in the transverse direction the length scale has been compressed by factor of 2; therefore the modulus at first glance seems to be circularly symmetric (i.e., spherically symmetric in space) in spite of the Fitzgerald-Lorentz contraction in the axial direction. Chosen values of the parameters are $b=2\pi/\lambda$ with $\lambda=1/4$ μm and $\beta=0.8$ or $\tilde{v}=1.25c$ (again, the plots remain the same with any other unit length instead of 1 μm).

$$\Psi(\rho,z,t)=\frac{\sin[b\sqrt{\rho^2+\gamma^2(z-vt)^2}]}{b\sqrt{\rho^2+\gamma^2(z-vt)^2}}\exp[ib\beta\gamma(z-\tilde{v}t)], \tag{22}$$

which gives a LW whose envelope moves rigidly along the z axis with the subluminal velocity $v=\beta c$, whereas the phase modulation moves superluminally with $\tilde{v}\equiv\beta^{-1}c=c^2/v$. In addition, its *sinc*-function-like amplitude distribution is no longer spherically symmetric as it was in the wave's rest frame. Instead, it has been compressed in the axial direction due to the Fitzgerald-Lorentz contraction; see Fig. 11. Equivalently, Eq. (22) can be obtained through the LT of coordinates in Eq. (19) [14], that proves our momentum-domain derivation. It is interesting to note that the pulse given by Eq. (22) was derived long ago by Mackinnon in another context of theoretical physics [49]. Salo *et al.* [50] calculated subsonic acoustical LWs inserting nonisotropic spectral functions into an equivalent of our Eq. (4). However, the spectra used have not resulted in closed-form expressions for the field. By consulting Fig. 10 it becomes obvious that any monochromatic field—including more or less narrow beams—must turn out to be a subluminal LW if observed in another reference frame. We have obtained an interesting beamed version of the Mackinnon's pulse from an anisotropic version of the wave given by Eq. (19) in which the origin had been shifted to an imaginary location $z_0=id$, i.e., the ''seed'' wave was the nonparaxial Gaussian beam (see Ref. [34] and references therein). The resulting field of such a new subluminal LW is given by the same closed-form expression of Eq. (22); however, in the roots the axial variable z is to be replaced by $z-id$.

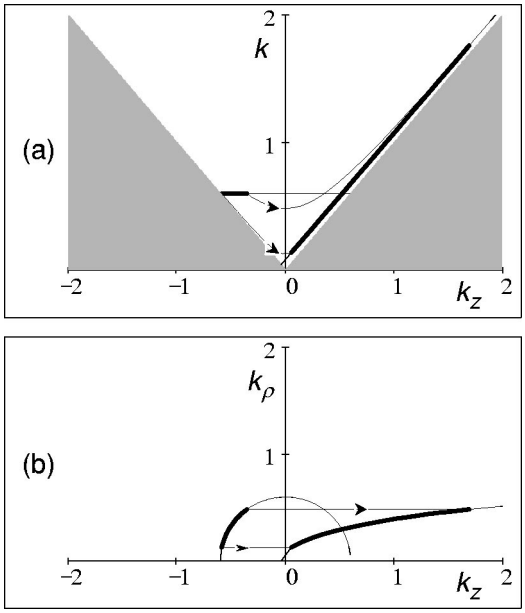

FIG. 12. Ultrarelativistic Lorentz transformation with $\beta=0.99$ of the support of a monochromatic beam into the support of a FWM-type luminal wave. The initial support (as observed in the frame K') corresponds to a beam, all plane-wave constituents of which have the same frequency $\omega/c=b=-0.5$ and propagation directions close to the negative direction of the z axis (see Fig. 10).

D. Luminal family—focus wave modes

Figure 12 depicts, in terms of the supports, how a monochromatic collimated beam, propagating in an ultrarelativistic frame in the negative direction of the z axis, in the laboratory frame turns out to be a wideband LW propagating almost luminally in the positive direction of the z axis. The closer the relative speed between the frames to the limit $\beta\rightarrow 1$, the closer the support to that of a luminal one is. Obviously, a luminal support line implies a δ function in the spectrum of Eq. (6) in the form $\delta(k-k_z-b)$ with $b>0$, which results from either a superluminal or subluminal case through an ultrarelativistic LT with $\beta\rightarrow 1$. If the initial wave (i.e., as observed in the moving frame) is taken to be monochromatic with a frequency $\omega'=cb'$, then according to Eq. (21) [also see Eq. (8)] the frequency must run to infinity as γ in order to retain the lateral structure and localization of the wave. Indeed, the δ factor in the form $\delta(k-k_z)$ would imply a degeneration of the parabolic support line in the (k_z,k_ρ) plane into straight starting from the origin, i.e., the support line would become that of a plane wave pulse propagating along the z axis. Let us take the spectrum in the laboratory frame with an exponential amplitude, i.e., in the form

$$\tilde{\Psi}(k_z,k)=\delta(k-k_z-b)\exp[-\Delta(k+k_z)]\Theta(k^2-k_z^2). \tag{23}$$

Inserting Eq. (23) into Eq. (4), carrying out the integration over k, and changing the variable $k_z\Rightarrow k_z-b/2$ results in the integral expression for the wave function:

$$\Psi(\rho,z,t)=\exp[-ib(z+ct)/2]\int_0^\infty dk_z\,J_0(\sqrt{2bk_z}\rho)$$
$$\times\exp(-2\Delta k_z)\exp[ik_z(z-ct)].$$

The integral is nothing but a known Laplace transform [see, e.g., Eq. 4.14(25) in Ref. [47]] and we finally obtain

$$\Psi(\rho,z,t)=\frac{\exp\{-\rho^2 b/2[2\Delta-i(z-ct)]\}}{[2\Delta-i(z-ct)]}$$
$$\times\exp[-ib(z+ct)/2], \tag{24}$$

which we recognize as the fundamental focus wave mode propagating in the positive direction of the z axis. Equation (24) coincides with the well-known expression of the FWM [12,14] if we complex conjugate Eq. (24) and change designations of the parameters $b/2\Rightarrow\beta'$ and $2\Delta\Rightarrow a_1$. Since the FWM has been studied in a large number of publications, here we omit plotting its spatial structure, all the more since it is quite similar to that of the FXW depicted in Fig. 7.

Equation (23) and Fig. 12 indicate the well-known circumstance in which the FWM is comprised not only of plane waves propagating into the positive hemisphere (i.e., those with $k_z>0$), but also of transversally propagating ones (with $k_z=0$ and $k_\rho=k=b$) as well as of backward propagating ones (with $k_z<0$). Due to the extremely strong Doppler effect and aberration when $\gamma\rightarrow\infty$ this is the case irrespective of how narrow (around the direction $-z$) the angular spectrum of the ''seed'' monochromatic beam in the K' frame is. Moreover, as shown in Ref. [6] the common monochromatic Gaussian beam propagating in the negative direction of the z axis, which only in the paraxial approximation satisfies the wave equation, transforms into the FWM in the laboratory frame in the limits $\beta\rightarrow 1$ and $\gamma\rightarrow\infty$. In this limit, as follows, e.g., from Eq. (7) and Fig. 12, in the laboratory frame one can get a luminal LW containing only forward-propagating optical-frequency constituents, if the monochromatic beam in the K' frame does *not* contain the most paraxial portion of the backward-propagating constituents (those with values $k_z'\simeq -k'$). In other words, for an optical-domain luminal LW in the laboratory frame its ''seed'' monochromatic beam in the ultrarelativistically moving frame K' has to be a backward-propagating Bessel beam with a small spread of k_ρ'.

In conclusion, no matter what the particular spectrum is—whether it covers with an exponential amplitude the whole possible length of the support line as in the case of the fundamental FWM or the amplitude is distributed around some point(s) of the line—the distinguishing common feature of all luminal LWs is that their support lies on a straight of slope 1 in the plane (k_z,k) and on a parabola in the space (k_z,k_ρ,k) (Fig. 3).

V. DISCUSSION AND CONCLUSIONS

The Lorentz transformation of LWs can be carried out either in the coordinate-time space or, equivalently, in the momentum-frequency space (we have used ''momentum'' as

a synonym for ''wave vector **k**'' for brevity, implying that the quantum terminology can be adopted for the LWs as well). The latter approach requires a bit more mathematical effort if the transformed spectrum is to be returned from the Fourier domain into the wave function in the $(\mathbf{r},t)$ representation. However, working in the momentum space with the Fourier(-Bessel) representation has certain advantages since it allows for better control and a physical insight into what is going on with the wave when the observer jumps into another inertial reference frame. We can easily track each plane-wave constituent (or Bessel-beam constituent) undergoing the Doppler shift and aberration. For example, from Fig. 5 and Sec. IV A. it is obvious that if the sign of k_{z0} of the ''seed'' cylindrical wave is positive, the FXW in the laboratory frame contains forward-propagating constituents only—i.e., is ''causal'' in the jargon adopted in the literature on LWs—while the presence of the backward-propagating constituents has been considered as a characteristic feature of the FXW. As to the task of finding new types of LWs, carrying out the subluminal LT on the spectral representation ensures that the result is really a source-free field everywhere, i.e., it consists of homogeneous-wave components and does not contain evanescent ones.

In contradistinction to the group velocity, the phase velocity cannot serve as a basis of classification of the LWs. Since all LWs have plane-wave constituents that propagate at angles θ $(0 \neq \theta \neq \pi)$ with respect to the z axis, the net phase velocity along the axis is necessarily larger than c, at least to a vanishingly small extent. Indeed, McKinnon's pulse has, according to Eq. (22), a phase velocity that in units of c is the reciprocal of its subluminal group velocity. The absolute value of the phase velocity along the axis for both the FXW and FWM's is almost exactly equal to c except in the vicinity of the moving center of the pulse, where it is slightly higher due to the Gouy-effect-type phase shift from $-\pi/2$ to $+\pi/2$, which follows from the denominator in both Eqs. (15) and (24). The superluminal LWs with a propagation-invariant wave function or X-type waves considered in Sec. IV B have a phase velocity equal to their superluminal group velocity, i.e., there is no dispersion since all the plane-wave constituents propagate at a fixed angle θ with respect to the z axis.

As far as axisymmetric LWs are considered, their supports in the three-dimensional momentum space (k_x,k_y,k_z) are surfaces of rotation: for superluminal LWs the support is a hyperboloid (which degenerates into a cone for X-type LWs), for subluminal LWs it is an ellipsoid, and for luminal LWs it is a paraboloid. As to more general cases of nonaxisymmetric waves—those possessing orbital angular momentum and bowtie beams [51] up to LWs in anisotropic media [52]—the support may lose its rotational symmetry, and possibilities to group such LWs into distinct classes each having a simple ''seed'' wave related through the LT needs further investigation.

As to practically feasible finite-aperture realizations of the LWs, the conclusions obtained remain valid since in the approach based on the spectral supports the condition of finite energy can be easily taken into account by allowing the support lines to acquire a finite thickness (as, in fact, it is depicted in the figures).

Despite the fact that we have considered scalar LWs here, the treatment and results hold *mutatis mutandis* for a vectorial electromagnetic field as well through the association of any scalar LW with components of the electromagnetic potential or the Hertz vector. For acoustic fields a somewhat intriguing operationalistic question arises concerning observations of LW in different reference frames: of course, an acoustic field—like any field obeying the wave equation—can be invariantly Lorentz transformed if the speed of sound is inserted into the formulas, but what is supposed to be the inertial frame in which we could observe the drastically changed wave? For an electromagnetic field, such question does not arise since there is no other speed involved than the universal constant c determining the fundamental properties of space and time. Let us stress that throughout this study if we say that a wave turns out to be quite different if *observed* in another reference frame, we do not mean that it simply seems different, we mean that it *is* different as verified by any appropriate physical means of measurement. All the more we do not mean what we can *see*, since, as is well known in the special theory of relativity, due to the finite speed of light *visible* shapes of relativistically moving objects are substantially distorted *in addition* to the Fitzgerald-Lorentz contraction. In fact, if we do not use indirect means like light scattering from small particles suspended in space, we see nothing if looking at the pulse from a side.

Apart from enabling a deeper comprehension of the physical nature of LWs and of the Lorentz transformation in wave optics in general, the present study might also be of practical significance, e.g., in finding new LWs with prescribed properties. Of course, transforming into a relativistically moving frame can hardly be viewed as a physical tool for the generation of a LW; however, it may be practically useful for a treatment of the interaction between relativistic particles and localized electromagnetic waves in research fields like laser-driven acceleration, etc.

ACKNOWLEDGMENTS

The authors are grateful to Amr Shaarawi (American University in Cairo) for stimulating discussions. The research was supported by the Estonian Science Foundation.

[1] J.N. Brittingham, J. Appl. Phys. **54**, 1179 (1983).
[2] A. Sezginer, J. Appl. Phys. **57**, 678 (1984).
[3] T.T. Wu and H. Lehmann, J. Appl. Phys. **58**, 2064 (1985).
[4] R.W. Ziolkowski, J. Math. Phys. **26**, 861 (1985).
[5] H.E. Moses and R.T. Prosser, IEEE Trans Antennas Propag. **AP-34**, 188 (1986).
[6] P.A. Bélanger, J. Opt. Soc. Am. A **3**, 541 (1986).
[7] P. Hillion, J. Math. Phys. **28**, 1743 (1987).

[8] E. Heyman, IEEE Trans. Antennas Propag. **AP-37**, 1604 (1989).
[9] P.L. Overfelt, Phys. Rev. A **44**, 3941 (1991).
[10] J. Lu and J.F. Greenleaf, IEEE Trans. Ultrason. Ferroelectr. Freq. Control **39**, 19 (1992).
[11] R. Donnelly, and R. Ziolkowski, Proc. R. Soc. London, Ser. A **440**, 541 (1993).
[12] R.W. Ziolkowski, I.M. Besieris, and A.M. Shaarawi, J. Opt. Soc. Am. A **10**, 75 (1993).
[13] W.A. Rodriguez and J.Y. Lu, Found. Phys. **27**, 435 (1997).
[14] I. Besieris, M. Abdel-Rahman, A. Shaarawi, and A. Chatzipetros, Prog. Electromagn. Res. **19**, 1 (1998).
[15] J. Salo, J. Fagerholm, A.T. Friberg, and M.M. Salomaa, Phys. Rev. E **62**, 4261 (2000).
[16] P. Saari, in *Time's Arrows, Quantum Measurement and Superluminal Behavior, Scientific Monographs: Phys. Sci. Series*, edited by D. Mugnai *et al.* (CNR, Rome, Italy, 2001), p. 37.
[17] E. Recami, M. Zamboni-Rached, K.Z. Nóbrega, C.A. Dartora, and H.E. Hernández, IEEE J. Sel. Top. Quantum Electron. **9**, 59 (2003).
[18] P. Saari and K. Reivelt, Phys. Rev. Lett. **79**, 4135 (1997).
[19] H. Sõnajalg, M. Rätsep, and P. Saari, Opt. Lett. **22**, 310 (1997).
[20] D. Mugnai, A. Ranfagni, and R. Ruggeri, Phys. Rev. Lett. **84**, 4830 (2000).
[21] I. Alexeev, K.Y. Kim, and H.M. Milchberg, Phys. Rev. Lett. **88**, 073901 (2002).
[22] R. Grunwald, V. Kebbel, U. Griebner, U. Neumann, A. Kummrow, M. Rini, E.T.J. Nibbering, M. Piché, G. Rousseau, and M. Fortin, Phys. Rev. A **67**, 063820 (2003).
[23] K. Reivelt and P. Saari, Phys. Rev. E **66**, 056611 (2002).
[24] P. Di Trapani, G. Valiulis, A. Piskarskas, O. Jedrkiewicz, J. Trull, C. Conti, S. Trillo, Phys. Rev. Lett. **91**, 093904 (2003).
[25] A.M. Attiya, E. El-Diwany, A.M. Shaarawi, and I.M. Besieris, Prog. Electromagn. Res. **30**, 191 (2000).
[26] A.M. Attiya, E. El-Diwany, A.M. Shaarawi, and I.M. Besieris, Prog. Electromagn. Res. **38**, 167 (2002).
[27] C. Conti and S. Trillo, Opt. Lett. **28**, 1251 (2003).
[28] S. Orlov, A. Piskarskas, and A. Stabinis, Opt. Lett. **27**, 2103 (2002).
[29] J. Durnin, J.J. Miceli, Jr., and J.H. Eberly, Phys. Rev. Lett. **58**, 1499 (1987).
[30] M. Zamboni-Rached, K.Z. Nóbrega, E. Recami, and H.E. Hernández-Figueroa, Phys. Rev. E **66**, 046617 (2002).
[31] C.J.R. Sheppard, J. Opt. Soc. Am. A **18**, 1579 (2001).
[32] A.P. Kiselev and M.V. Perel, J. Math. Phys. **41**, 1934 (2000).
[33] S.M. Feng, H.G. Winful, and R.W. Hellwarth, Phys. Rev. E **59**, 4630 (1999).
[34] P. Saari, Opt. Express **8**, 590 (2001).
[35] R. Piestun and J. Shamir, J. Opt. Soc. Am. A **15**, 3039 (1998).
[36] Z. Bouchal and R. Horák, J. Mod. Opt. **48**, 333 (2001).
[37] K. Reivelt, Opt. Express **10**, 360 (2002).
[38] K. Reivelt and P. Saari, in *Ultrafast Processes in Spectroscopy*, *Proceedings of the X International Symposium*, edited by R. Kaarli, A. Freiberg, and P. Saari (Institute of Physics, Tartu, Estonia, 1998), p. 168.
[39] K. Reivelt and P. Saari, J. Opt. Soc. Am. A **17**, 1785 (2000).
[40] K. Reivelt and P. Saari, J. Opt. Soc. Am. A **18**, 2026 (2001).
[41] K. Reivelt and P. Saari, Phys. Rev. E **65**, 046622 (2002).
[42] K. Reivelt and P. Saari, physics/0309079.
[43] H. Sõnajalg and P. Saari, Opt. Lett. **21**, 1162 (1996).
[44] A.O. Barut, G.D. Maccarrone, and E. Recami, Nuovo Cimento A **71**, 509 (1982).
[45] A.O. Barut and A.C. Chandola, Phys. Lett. A **180**, 5 (1993).
[46] J. Lu, H. Zou, and J.F. Greenleaf, IEEE Trans. Ultrason. Ferroelectr. Freq. Control **42**, 850 (1995).
[47] H. Bateman and A. Erdély, *Tables of Integral Transforms* I (McGraw-Hill, New York, 1954).
[48] V.V. Borisov and A.P. Kiselev, Appl. Math. Lett. **13**, 83 (2000).
[49] L. Mackinnon, Found. Phys. **8**, 157 (1978).
[50] J. Salo and M.M. Salomaa, Acoust. Res. Lett. Online **2**, 31 (2001).
[51] J. Lu, IEEE Trans. Ultranson. Ferroelectr. Freq. Control **42**, 1050 (1995).
[52] J. Salo, J. Fagerholm, A.T. Friberg, and M.M. Salomaa, Phys. Rev. Lett. **83**, 1171 (1999).